Available online at www.sciencedirect.com
SCIENCE DIRECT®

Journal of the European Ceramic Society 23 (2003) 2849–2856
www.elsevier.com/locate/jeurceramsoc

High-temperature mechanical properties of zirconia/nickel composites

A. Morales-Rodríguez[a], A. Bravo-León[a], A. Domínguez-Rodríguez[a], S. López-Esteban[b], J.S. Moya[b], M. Jiménez-Melendo[a,*]

[a]*Departamento de Física de la Materia Condensada, Universidad de Sevilla, Aptdo. 1065, 41080 Sevilla, Spain*
[b]*Instituto de Ciencias de Materiales, CSIC, Cantoblanco, 28049 Madrid, Spain*

Abstract

The creep properties of wet-processed 3 mol% yttria-stabilized tetragonal zirconia (YTZP)–nickel cermets have been studied for metal concentrations of 20 and 40 vol.% (below and above, respectively, the percolation threshold). Compressive creep tests were performed at constant load at temperatures ranging from 950 to 1250 °C and under stresses between 5 and 100 MPa. The experimental results have been correlated with microstructural observations by scanning and transmission electron microscopy. Similar values of the stress exponent n and the activation energy for flow Q were found for the two metal contents studied. Both creep parameters decrease when increasing the stress and/or the temperature. This trend is similar to that exhibited by high-purity monolithic YTZP, indicating that the overall creep behavior of the composites is primarily controlled by the matrix phase. The strain rate of 40 vol.% Ni cermet is one order of magnitude higher than that of 20 vol.% Ni cermet. The mechanical properties of the composites is discussed in terms of a creep model for two-phase materials.

Keywords: Cermet; Creep parameters; Nickel; Plasticity; Zirconia

1. Introduction

In the last few years, materials formed by a ceramic matrix with a metallic phase (''cermets'') have received increasing attention because of their singular mechanical, electrical and magnetic properties. These composites have been proposed as excellent candidates for structural and high added-value functional applications related to aerospace industry, energy conversion, sensors and transductors.[1,2] In particular, the zirconia/nickel system is of interest for temperature and flow sensors, and especially as super-thermal protectors for gas turbines and supersonic propulsion systems of spacecrafts.[3] It is currently used as anode configurations for solid oxide fuel cells (SOFC).[4]

Zirconia/nickel composites have a good compatibility because of their similar thermal expansion coefficients and elastic moduli; also, the melting temperature of nickel (1455 °C) is above the sintering temperature of zirconia. The electrical behavior of wet-processed tetragonal zirconia/nickel composites have been recently characterized by complex impedance measurements as a function of the nickel content.[5] It was found that the percolation threshold appeared at a critical value of 0.34 vol.% Ni; the dielectric constant reached a value as high as 1000 at this metal concentration. The percolation threshold for the zirconia/nickel system is much higher than the limit predicted by the classic percolation theory for disordered systems (0.16 vol.%).[6] The existence of a first-neighbor ordering between nickel particles was suggested by the authors.[5]

In order to take full advantage of these properties for potential applications, it is essential to characterize the mechanical behavior of the zirconia/nickel system. However, only one study has explored the mechanical behavior of these cermets at room temperature,[7] and there are no data at elevated temperatures. At room temperature, a decrease in flexural and tensile resistance, and in toughness, was found when increasing nickel content. The progressive loss of mechanical performance with metal concentration was attributed to the weak bond between nickel particles and zirconia grains.[7]

The main objective of the present work is therefore to investigate the high-temperature plastic deformation of

* Corresponding author. Tel.: +34-95-455-2891; fax: +34-95-461-2097.

0955-2219/03/$ - see front matter © 2003 Elsevier Ltd. All rights reserved.
doi:10.1016/S0955-2219(03)00309-1

wet-processed zirconia/nickel cermets. The mechanical behavior was evaluated at two metal contents below and above the percolation limit, and comparisons made with the monolithic constituents.

2. Experimental procedure

2.1. Material fabrication

The materials used in this study, supplied by the ICMM (Instituto de Ciencia de Materiales, Madrid, Spain), were fabricated by a wet process described in detail elsewhere.[8] A mixture of powders was used as the starting material: 3 mol% Y_2O_3-stabilized ZrO_2 (YTZP) with >99.98% purity, and nickel powder with >99.9% purity and average particle size of 400 nm. However, metallic particles formed welded aggregates of larger size (~1 μm), which controlled their final rheological behavior.

Stable aqueous suspensions of YTZP and Ni, with 70 wt.% solids loading, were prepared with relative nickel concentrations of 20 and 40% in volume (labeled Ni20 and Ni40 in the following for the sake of brevity). The mixtures were milled with zirconia balls for 24 h and then hot dried at 90 °C. Finally, the powders were isostatically pressed at 200 MPa. The resulting bars were fired in reductor atmosphere (90% Ar/10% H_2) in two steps: first, at 500 °C for 2 h in order to reduce the NiO present in the surface of the starting nickel particles; second, at 1400 °C for 2 h for final sintering. The heating/cooling rate was kept at 600 °C/h. Monolithic YTZP was synthesized by the same technique for comparison. The bulk densities of the composites, measured by Archimedes' method, were about 90% of the respective theoretical values.

2.2. Mechanical tests and microstructural observations

Rectangular specimens of 4×3×3 mm^3 in size were cut from the as-received materials for mechanical tests. Compressive experiments were carried out in argon atmosphere at temperatures T between 950 and 1250 °C under constant load in a creep machine, at nominal stresses σ ranging from 5 to 100 MPa. Deformation was continuously monitored during the test using an extensometer. The recorded data, variation of the specimen length vs. time, were plotted as log $\dot{\varepsilon}$–ε curves (creep curves), where $\dot{\varepsilon}$ and ε are the strain rate and the true strain, respectively. Creep curves were analyzed using the standard high-temperature power law for steady-state deformation:[9]

$$\dot{\varepsilon} = A \cdot \sigma^n \cdot d^{-p} \cdot \exp(-Q/RT) \quad (1)$$

where A is a constant, n the stress exponent, p the grain size exponent, Q the activation energy for flow and R the gas constant. Stress and temperature changes were performed during a creep test in order to deduce the values of n and Q, respectively, which depend on the details of the deformation mechanism.

The microstructural characterization of the as-received and deformed composites was carried out using scanning electron microscopy (SEM, Microscopy Service, University of Sevilla, Spain). To this end, sections were cut from the samples (parallel to the load axis in the case of strained specimens) and mechanically polished finishing with diamond paste of 1 μm-grade. The sections were then thermally etched at 1250 °C for 30 min in reductor atmosphere (90% Ar/10% H_2). The morphological parameters of the different phases were characterized by using a semiautomatic image analyzer. The microstructure of the samples was also examined by transmission electron microscopy (TEM). Thin foils were obtained following a classical procedure of grinding and ion thinning of sliced sections.

3. Experimental results

3.1. Microstructure of as-received materials

Fig. 1 shows SEM micrographs of Ni20 and Ni40 composites. Metallic particles (bright phase) are homogeneously distributed throughout the zirconia matrix (dark phase). As can be seen, nickel particles are well isolated from each other in Ni20 (Fig. 1a), whereas some contact between neighbor particles can be found in Ni40 (Fig. 1b). This fact agrees with results of electrical measurements in the same composites,[5] which set the percolation limit for a nickel content of 34 vol.%. Metal particles are almost spherical, with an average grain size d_{Ni} (taken as the equivalent planar diameter $d=[4(\text{grain area})/\pi)^{1/2}]$) of 0.8±0.1 μm in Ni20 and 1.1±0.1 μm in Ni40. The slight difference between both values is probably due to the overlapping between the individual nickel particles in the Ni40 cermet, which makes the size measurements difficult.

The thermal etching used to reveal the microstructure is responsible for the growth by evaporation of the metallic particles placed on the polished surfaces (Fig. 1), giving an apparent porosity higher than the true one. Pores are systematically associated with nickel particles, and smaller in size. This pore distribution is not due, however, to thermal etching because the same distribution was observed on non thermal-etched polished samples.

On the other hand, the zirconia matrix (Fig. 2) exhibits equiaxed grains with an average grain size $d_{YTZP}=0.13\pm0.01$ μm for both YTZP/Ni composites. The same morphology was found in monolithic TZP processed by the same route than the cermets, except for a larger grain size (0.22±0.01 μm). It is known that the

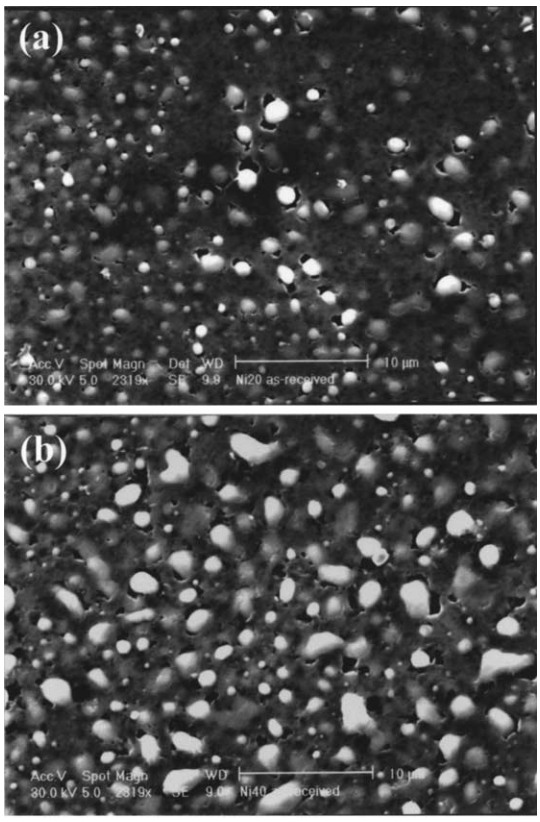

Fig. 1. SEM micrographs of as-received Ni20 (a) and Ni40 (b) composites. Nickel particles (bright phase) are homogeneously distributed throughout the YTZP matrix. Some overlapping between neighbor nickel particles occurs in Ni40.

Fig. 2. SEM micrograph of Ni20 showing the fine-grained microstructure of the zirconia matrix.

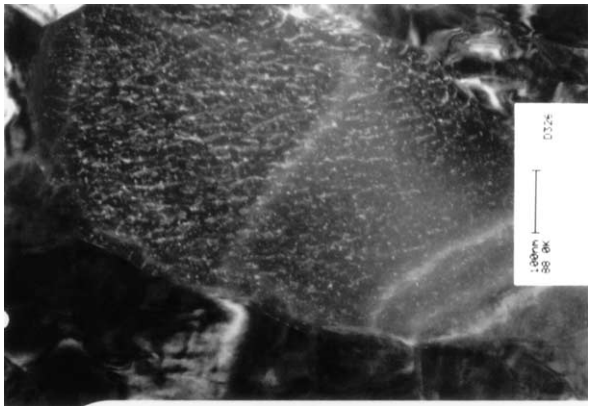

Fig. 3. TEM micrograph showing a nickel particle surrounded by zirconia grains.

addition of secondary phases to ceramic materials usually reduces the grain growth.[10–12]

TEM observations (Fig. 3) showed the absence of dislocations and other kind of defects in the zirconia grains and metal inclusions, though these latter ones were occasionally twinned. Clean YTZP–Ni and YTZP–YTZP grain boundaries were observed in all the cases (at least up to maximum TEM resolution used, ×115k). This result shows the high quality of the fabrication process, that reduces completely the oxide layer of the original metal particles.

3.2. High temperature mechanical behavior

Fig. 4 shows the log $\dot{\varepsilon}$–ε curves for Ni20 (Fig. 4a) and Ni40 (Fig. 4b) composites obtained at 1200–1250 °C under stresses between 3 and 14 MPa. A prominent transient creep appears upon the first loading (probably due to a densification process), followed by steady-state stages characterized by an almost constant slope. No evidence of specimen failure was found at the strains studied ($\varepsilon \sim 45\%$).

The stress exponent n and the activation energy Q were determined by changing σ or T during the tests (Fig. 4). The maintenance of the strain rate levels after positive and negative temperature changes indicates that no grain growth took place during deformation. Average values of $n = 4.0 \pm 0.4$ and $Q = 610 \pm 20$ kJ/mol where found for Ni20 (Fig. 4a). Similar results ($n = 3.9 \pm 0.1$ and $Q = 640 \pm 50$ kJ/mol) where estimated for Ni40 tested under identical experimental conditions (Fig. 4b). The values of n are in rough agreement with the slopes of the log $\dot{\varepsilon}$–ε curves, indicating a rather homogeneous deformation of the specimens.[13] Regarding the absolute values of the strain rate, Ni40 is faster in more than one order of magnitude than Ni20.

Fig. 5 shows the creep curve for Ni20 deformed at 1200–1250 °C and larger stresses (32–66 MPa). The creep parameters are $n = 2.8 \pm 0.3$ and $Q = 490 \pm 50$ kJ/mol, smaller than those found at lower stresses (Fig. 4a). Intermediate values ($n = 3.5 \pm 0.2$, $Q = 550 \pm 30$ kJ/mol) were estimated at stresses between 15 and 25 MPa at the same temperatures. This trend (i.e. both n and Q decrease with increasing the stress at a given temperature) was also observed in Ni40 composites.

In order to study the dependence of the creep parameters with temperature, mechanical tests were performed at lower temperatures. Again the stress exponent and the activation energy increased with

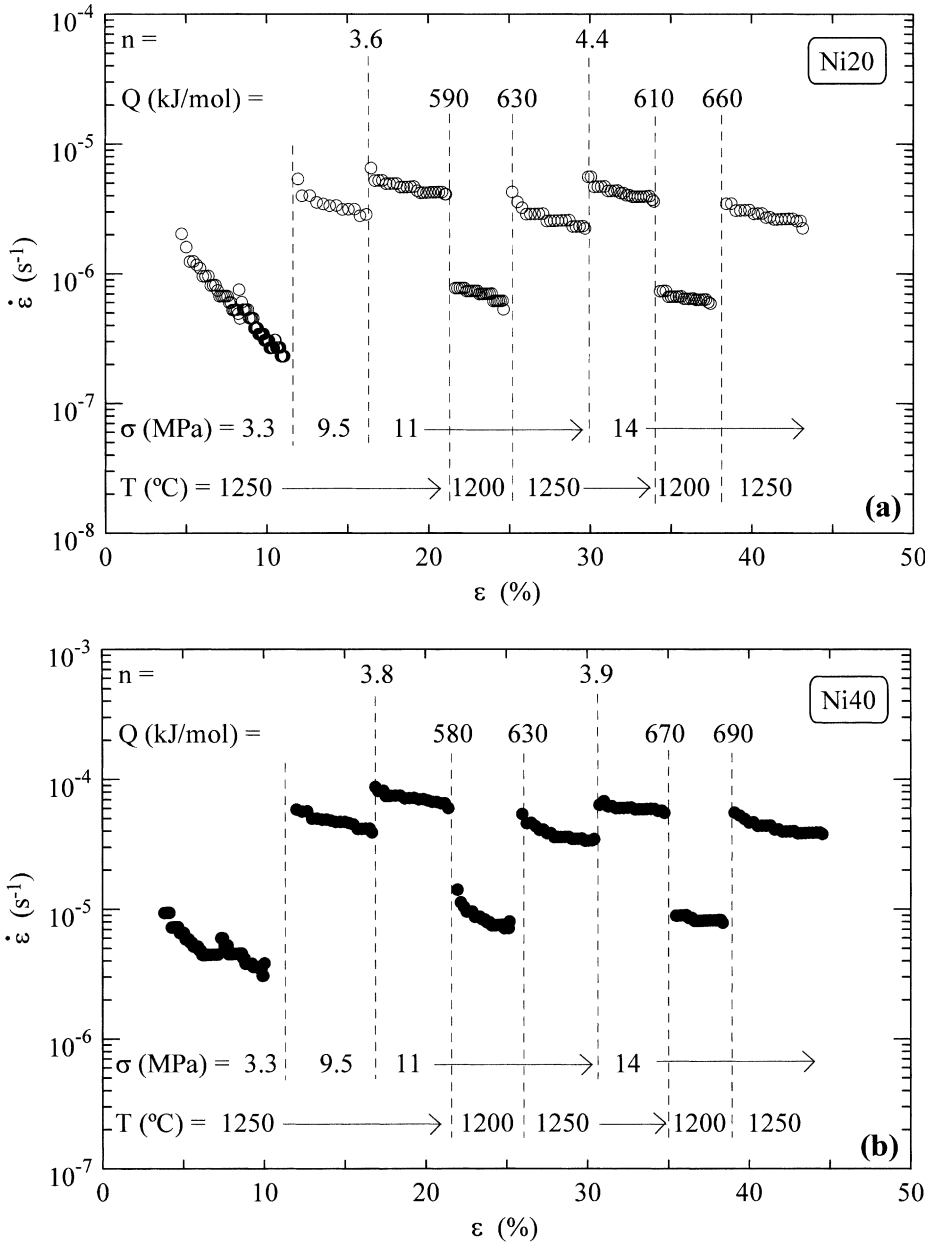

Fig. 4. Creep curves plotted as log $\dot{\varepsilon}$ vs ε at 1200–1250 °C and low stresses for Ni20 (a) and Ni40 (b). Several determinations of the stress exponent n and the activation energy Q by stress and temperature changes are shown.

respect to the values found at higher temperatures under similar stresses. For example, values of $n=4.9\pm0.4$ and $Q=670\pm30$ kJ/mol were estimated for Ni40 between 1150 and 1200 °C at intermediate stresses (13–22 MPa).

Because of the enhanced plasticity of the cermets, especially in Ni40, relatively fast strain rates were found even at temperatures as low as 1000 °C. Fig. 6 displays a creep curve for Ni40 between 1050 and 950 °C strained up to $\varepsilon=50\%$; strain rates are typically about 10^{-5} s^{-1} under these experimental conditions. It should be noted that no creep data for zirconia-based ceramics have been reported at temperatures below about 1100 °C. Regarding the creep parameters, it was found that $n=2.5\pm0.1$ and $Q=640\pm30$ kJ/mol.

3.3. Microstructure after deformation

The microstructure of the composites was investigated after deformation, looking for modifications in grain features and for the presence of dislocations and other defects. Fig. 7 shows the microstructure of the Ni20 (Fig. 7a) and Ni40 (Fig. 7b) composites deformed at 1200–1250 °C and low stresses to a final strain $\varepsilon=45\%$ (Fig. 4). Grain size and shape measurements of the zirconia grains indicate that no changes occurred during deformation. In contrast, nickel particles acquired an acicular shape with the major diameter perpendicular to the direction of the applied stress, though keeping the same particle size (i.e. the same particle area). By mea-

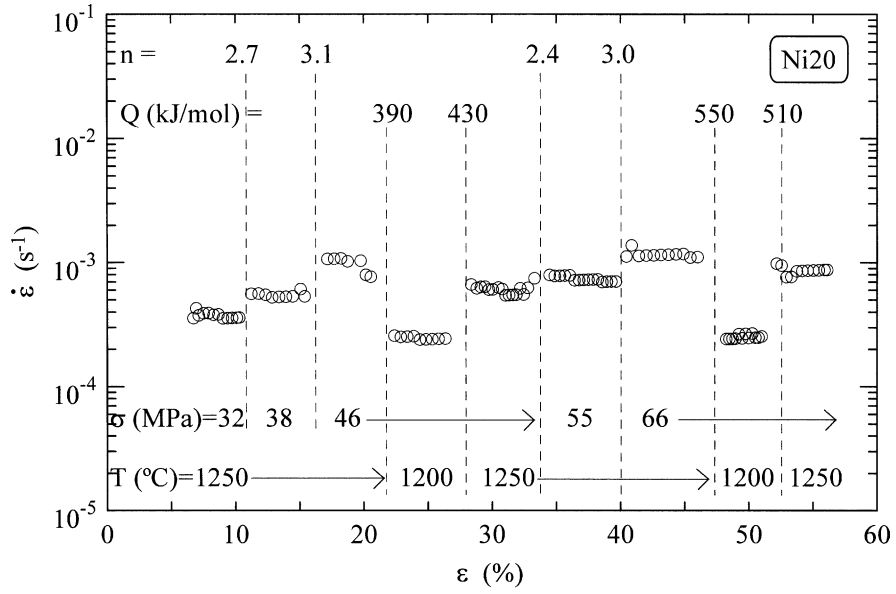

Fig. 5. Log $\dot{\varepsilon}$ vs ε curve for Ni20 at 1200–1250 °C and high stresses.

suring the maximum and minimum diameters, an average particle deformation of about 35% was estimated. Similar results were found at the other experimental conditions studied.

TEM observations of deformed samples showed the same features indicated previously for the as-received materials: both phases were free of dislocations, twinning of the nickel particles in the same proportion than prior to deformation, and absence of secondary phases along the grain boundaries.

4. Discussion

In order to elucidate the deformation mechanisms operating in the composites, it is necessary to discuss previously the creep behavior of the starting monolithic materials, YTZP and Ni. Tetragonal zirconia polycrystals exhibit superplasticity (i.e., reach $\epsilon > 100\%$ before failure) at high temperatures (1250–1500 °C); grain boundary sliding has been recognized as the primary deformation mechanism. Reviews of creep data in this material[10,14–16] have shown a strong dependence with the impurity content. For low-purity materials (residual impurity content above about 0.1 wt.%), a single rate-controlling mechanism exists over the entire stress and temperature ranges, characterized by $n=2$ and $Q=460$ kJ/mol; these values are compatible with grain boundary sliding accommodated by lattice diffusion of cations.[10,13] In contrast, high-purity materials (residual impurity content below 0.1 wt.%) exhibit a complex behavior: n and Q increase continuously from 2 and 460 kJ/mol, respectively, up to 5 and 700 kJ/mol when decreasing the stress and/or the temperature; a further change towards $n=1$ was found at the lowest stresses studied. Such an evolution of the creep parameters was interpreted in terms of a single deformation process that incorporates a threshold stress, below which grain boundary sliding does not contribute to strain.[10,13] A few compressive creep tests were conducted at 1250 °C on monolithic zirconia fabricated by the same technique as the cermets. The strain rates fall over the "high-purity" behavior (Fig. 8), as could be expected from the high purity of the starting zirconia powder.

On the other hand, creep data for monolithic polycrystalline nickel[19] show that, in the experimental conditions used in this work ($\sigma=1$–100 MPa, $T=1000$–1250 °C and d ~ 1 μm, corresponding to the size of the metallic particles in the cermets), the creep parameters are $n=1$ and $Q=115$ kJ/mol. Such values were associated with a diffusional flow mechanism controlled by boundary diffusion (Coble creep). There is a transition towards $n \sim 5$ and $Q=280$ kJ/mol as the stress and/or the temperature increase due to the activation of a dislocation recovery-controlled creep mechanism. In any case, typical strain rates are above 10^{-2} s^{-1}, significantly higher than those of monolithic zirconia.

The values of n and Q found in YTZP/Ni composites are similar to those noted above for high-purity monolithic zirconia, and follow the same complex trend with stress and temperature. This result, along with the independence of n and Q with nickel content (Fig. 4), suggests that the high-temperature plastic deformation of the cermets is controlled primarily by the zirconia matrix, which still retains its "high-purity" behavior despite the metal addition. This agrees with TEM observations regarding the absence of secondary phases along grain boundaries.

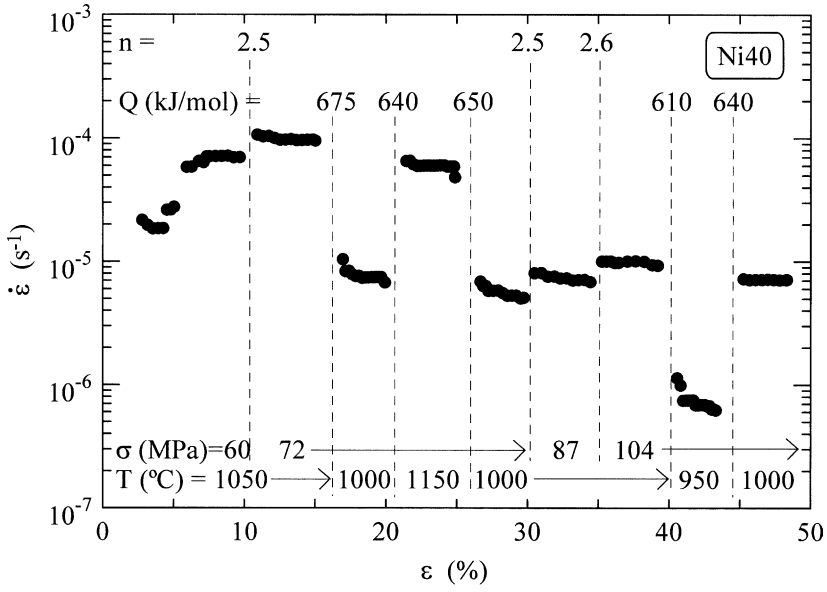

Fig. 6. Log $\dot{\varepsilon}$ vs ε curve for Ni40 deformed between 1050 and 950 °C under high stresses. Relatively high strain rates were found at these low temperatures.

The overall strain rates of the composites fall in between those of monolithic zirconia and monolithic nickel, and they depend on nickel content. Fig. 8 displays the variation of grain size-compensated $\dot{\varepsilon}$ with σ at 1250 °C for monolithic YTZP and Ni20 and Ni40 composites. Because of the difference in grain size, the deformation rates have been corrected with d by assuming that zirconia is the rate-controlling phase in the composites; a value of $p=2$[10] has been used in Eq. (1) for such a normalization. As can be seen, the strain rate of Ni20 is about twice as much as that of monolithic zirconia, increasing up to a factor of 30 for Ni40.

Creep data for high-purity YTZP at temperatures below 1250 °C are very scarce and show a large dispersion,[20] that make difficult the comparison with the cermets. The most remarkable result at these low temperatures is the relatively large ductility exhibited by the cermets, even at 950 °C (Fig. 6), without evidence of internal failure.

French et al. [21] have developed a creep model for duplex microstructures by assuming that the strain and the strain rate (isostrain configuration) or the stress (isostress configuration) are the same for each phase. The flow of each phase and that of the composite material is defined by its own constitutive creep equation [Eq. 1]. Because of the large difference in deformation rates of the two constituent monoliths, this model predicts that the composite strain rate will be controlled by the soft phase (nickel) for the isostress case and by the hard phase (YTZP) for the isostrain case. The first condition can be ruled out in this study since the creep parameters n and Q in the composites, as well as the absolute values of the strain rate, are very different of those reported in nickel.

For the isostrain configuration, the overall composite stress σ_c is given by the relation:[21]

$$\sigma_c = V_{YTZP}\sigma_{YTZP} + V_{Ni}\sigma_{Ni} \quad (2)$$

where V is the volume fraction and σ the stress supported by each phase in the composite. Following the previous reasoning, this expression can be simplified to:

$$\sigma_c \cong V_{YTZP}\sigma_{YTZP} \quad (3)$$

indicating that the stress supported by the zirconia phase σ_{YTZP} in the composite would be higher ($V_{YTZP}=0.8$ in Ni20 and 0.6 in Ni40) than the applied stress σ_c, and increases with increasing the metal content. From Eq. (3), and by taking $n=3$–4 (at 1250 °C, Figs. 4 and 5), the overall composite creep rate is predicted to be $\dot{\varepsilon}_c \cong 2\dot{\varepsilon}_{YTZP}$ for Ni20 and $\cong 7\dot{\varepsilon}_{YTZP}$ for Ni40, with $\dot{\varepsilon}_{YTZP}$ the strain rate of monolithic zirconia. The first result reproduces correctly the increase in deformation rate found experimentally in Ni20, but the second one is lower than the enhancement factor obtained in Ni40 (Fig. 8).

The isostrain model is consistent with the microstructural features observed in deformed samples. This configuration assumes that both phases undergo the same deformation, and equals the specimen strain. As noted above, zirconia grains easily slide on each other along their grain boundaries, giving large macroscopic strains without significant microstructural changes. On the other hand, the lack of dislocation activity within the metal particles is consistent with the Coble creep mechanism proposed for nickel.[19] Furthermore, this model predicts that the individual particles will suffer approximately the same strain as that of the specimen as a whole. Such an elongation of the metal inclusions has

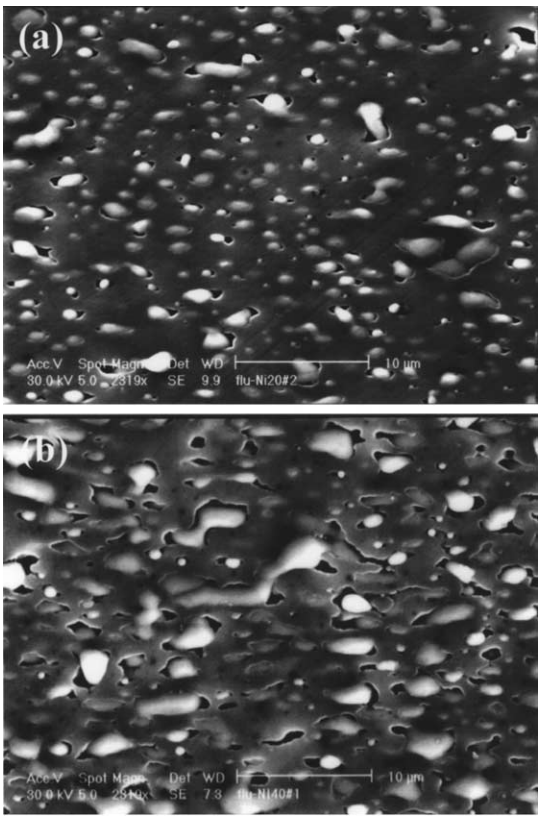

Fig. 7. SEM micrographs of Ni20 (a) and Ni40 (b) cermets strained up to $\varepsilon = 45\%$ (Fig. 4). Loading axis is vertical. Nickel particles have a disk-like shape with the maximum diameter perpendicular to the applied stress.

been systematically observed in the strained composites (Fig. 7); the average deformation of the nickel phase (~35%) roughly agrees with the sample deformation (~45%).

It can be concluded that nickel additions to zirconia promote an increase in creep rate due to the reduction of the effective surface that supports load. The isostrain model accounts for both the mechanical and microstructural features observed in Ni20 composites, where the zirconia grains form a continuous skeleton that completely surrounds the individual nickel particles and thus being capable of supporting load. In this regard, it seems that clean zirconia/nickel interfaces are unlikely to play any role in the high-temperature mechanical properties of the composites, as was also concluded at room temperature.[7] The breakdown of the analysis based on the isostrain series elements in Ni40 composites can be explained taking into account the overlapping of the metal particles at this nickel concentration, which exceeds the percolation threshold. The interconnection of the softer phase may act as local short-circuits for deformation, leading to average creep rates faster than those predicted by the simple isostrain model. This point is presently the subject of further investigation.

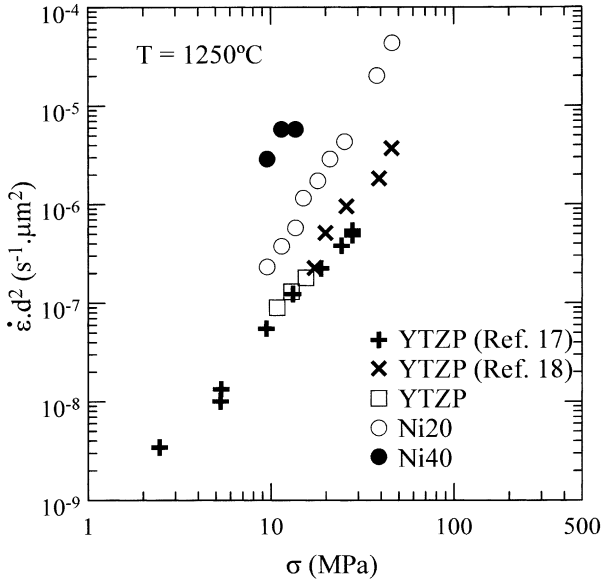

Fig. 8. Variation of grain size-compensated strain rate with stress at 1250 °C for high-purity monolithic zirconia reported in the literature,[17,18] along with the results obtained in this work in Ni20 and Ni40 composites and monolithic YTZP.

5. Conclusions

The high-temperature mechanical properties of wet-processed YTZP/Ni composites with nickel contents of 20 and 40 vol.% have been investigated under compression at constant load in the temperature range 950–1250 °C. The composites consist of large nickel inclusions (1 μm in size) uniformly distributed throughout a fine-grained zirconia matrix (0.13 μm in size).

The stress exponent n and the activation energy for flow Q are similar for both metal concentrations and display the variation observed in high-purity monolithic zirconia, indicating that the ceramic matrix controls the creep behavior of the composites. Metal addition results in large ductilities even at temperatures as low as 950 °C. A simple isostrain creep model for duplex microstructures predicts correctly the creep rate and microstructural features observed in Ni20 composites. However, it fails to account for the deformation rate in Ni40 composites. The overlapping between individual nickel particles at this metal concentration, greater than the percolation threshold, may be responsible for the discrepancies. Clean zirconia/nickel interfaces do not seem to play any role in the mechanical behavior of the composites.

Acknowledgements

This research has been supported by CICYT No. MAT 2000-1117 (Ministerio de Ciencia y Tecnología, Madrid, Spain).

References

1. Reschke, S. and Bodganow, C., Engineering ceramics: new perspectives through value-added (multi-) functionality. *Key Eng. Materials*, 1999, **175-176**, 1–10.
2. Sundeen, J. E. and Buchanan, R. C., Electrical properties of nickel–zirconia cermet films for temperature- and flow-sensor applications. *Sensor. Actuators A-Phys.*, 1997, **63**(1), 33–40.
3. Kuroda, Y., Kusaka, K., Moro, A. and Togawa, M., Functionally Gradient Materials. *Ceramic Transactions*, 1993, **34**, 271–278.
4. Heinrich, J. G. and Aldinger, F., *Ceramic Materials and Components for Engines*. Wiley-VCH, Weinheim, Germany, 2001.
5. Pecharromán, C., López-Esteban, S., Bartolomé, J. F. and Moya, J. S., Evidence of nearest-neighbor ordering in wet-processed zirconia-nickel composites. *J. Am. Ceram. Soc.*, 2001, **84**(10), 2439–2441.
6. Kirkpatrick, S., Percolation and conduction. *Rev. Mod. Phys.*, 1973, **45**(4), 574–588.
7. López-Esteban, S., Bartolomé, J. F., Moya, J. S. and Tanimoto, T., Mechanical performance of 3Y-TZP/Ni composites: tensile, bending and uniaxial fatigue tests. *J. Mater. Res.*, 2002, **17**(7), 1592–1600.
8. López-Esteban, S., Procesamiento, caracterización eléctrica y mecánica de materiales compuestos 3Y-TZP/Ni. PhD thesis, Universidad Politécnica de Madrid, 2001.
9. Poirier, J. P., *Creep of Crystals: High-temperature Deformation Processes in Metals, ceramics and minerals*. Cambridge University Press, Cambridge, UK, 1985.
10. Jiménez-Melendo, M., Domínguez-Rodríguez, A. and Bravo-León, A., Superplastic flow of fine-grained yttria-stabilized zirconia polycrystals: constitutive equation and dformation mechanisms. *J. Am. Ceram. Soc.*, 1998, **81**(11), 2761–2776.
11. French, F. D., Harmer, M. P., Chan, H. M. and Miller, G. A., Coarsening-resistant dual-phase interpenetrating microstructures. *J. Am. Ceram. Soc.*, 1990, **73**(8), 2508–2510.
12. Lange, F. and Hirlinger, M., Grain growth in two-phase ceramics: Al_2O_3 Inclusions in ZrO_2. *J. Am. Ceram. Soc.*, 1987, **70**(11), 827–830.
13. Jiménez-Melendo, M. and Domínguez-Rodríguez, A., Like-metal superplasticity of fine-grained Y_2O_3-stabilized zirconia ceramics. *Phil. Mag. A*, 1999, **79**(7), 1591–1608.
14. Carry, C., High ductilities, superplastic behaviors, and associated mechanisms in fine-grained ceramics. In *Proceedings of the M.R.S. International Meeting on Advanced Materials. "Superplasticity"*, ed. M. Kobayashi and F. Wakai. Materials Research Society, Pittsburg, PA, 1989, pp. 199–215.
15. Chokshi, A. H., Superplasticity in fine-grained ceramic and ceramic composites: current understanding and future prospects. *Mater. Sci. Eng. A*, 1993, **166**, 119–133.
16. Langdon, T. G., The characteristics of superplastic-like flow in ceramics. In *Plastic Deformation of Ceramics*, ed. R. C. Bradt, C. A. Brookes and J. L. Routbort. Plenum Press, New York, 1995, pp. 251–268.
17. Wakai, F., Sakaguchi, S. and Matsuno, Y., Superplasticity of yttria-stabilized tetragonal ZrO_2 polycrystals. *Adv. Ceram. Mater.*, 1986, **1**, 259–263.
18. Hermansson, T. and Dunlop, G. L., A high-temperature tensile testing rig for ceramic materials. *Int. J. High Technol. Ceram.*, 1988, **4**, 263–268.
19. Frost, H. J. and Ashby, M. F., *Deformation mechanism maps: the plasticity and creep of metals and ceramics*. Pergamon Press, Oxford, UK, 1982.
20. Gutiérrez-Mora, F., Domínguez-Rodríguez, A. and Jiménez-Melendo, M., Plasticity of nanocrystalline YTZP. *J. Eur. Ceram. Soc.*, 2002, **22**(14-15), 2615–2620.
21. French, J. D., Zhao, J., Harmer, M. P., Chan, H. M. and Miller, G. A., Creep of duplex microstructures. *J. Am. Ceram. Soc.*, 1994, **77**(11), 2857–2865.